Journal of Sound and Vibration (2002) **249**(3), 622–633
doi:10.1006/jsvi.2001.3740, available online at http://www.idealibrary.com on IDEAL®

PRELIMINARY COMPUTATIONS FOR CHATTER CONTROL IN END MILLING

S. E. Semercigil and L. A. Chen†

Faculty of Engineering and Science (*Mechanical Engineering*), *Victoria University of Technology*, *Footscray Campus*, *P.O. Box* 14428, *MCMC*, *Melbourne*, *Victoria* 8001, *Australia*.
E-mail: *Eren.Semercigil@vu.edu.au*

(*Received* 7 *September* 1998, *and in final form* 8 *June* 2000)

1. INTRODUCTION

Possibility of machine-tool chatter is a critical consideration when planning metal-cutting processes. Chatter is the excessive vibrations of the cutting tool relative to the workpiece. It causes a rough surface finish and dimensional inaccuracy of the work. In addition, excessive vibrations accelerate the wear of the cutting tool and the structural components. Hence, without a good understanding of the chatter phenomenon, an automated manufacturing process is not possible.

Tool chatter has long been a topic of significant interest. Research has been concentrated largely on estimating the cutting conditions to avoid the occurrence of chatter [1–6]. Control has been suggested with variable cutting speed, with specially designed cutter shapes and with on-line monitoring of the cutting conditions [2, 7, 8]. Efforts have also been made by exaggerating the process damping mechanism and by structural control of the cutter's parameters to avoid chatter [9]. However, if the cutting conditions are severe enough, tool chatter is virtually unavoidable [2, 7–9].

The approach taken in this study is to simply accept the presence of dynamic cutting forces which, if not controlled, are able to initiate excessive resonant vibrations of the cutting tool. Then the problem becomes one of designing a vibration controller to attenuate the excessive vibrations of the cutting tool which is in direct contact with the workpiece. Tool chatter is inherently a self-excited vibration problem. Vibrations of the tool affect the amplitude and the frequency content of the cutting (exciting) force. Therefore, it may be possible to avoid the initiation of the chatter instability, if this feedback loop could somehow be broken by attenuating the vibrations of the cutting tool.

Use of a passive vibration controller, an impact damper, is suggested to reduce the excessive vibrations of the end-mill cutter. Simulations will be presented for a case where the machine structure holding the cutter and the workpiece are rigid. The milling cutter is the only source of flexibility in the system. An impact damper will be incorporated in the flexible cutter. End-milling process is chosen deliberately due to its versatility and wide range of applications from aerospace industry to small prototype shops. Any improvement in this process will result in significant savings in manufacturing time and cost.

Next, a simple feedback model between the cutting force and oscillations of the tool will be presented. Then, the numerical procedure and the simplifying assumptions will be

†Now with IBM Canada Ltd., 844 Don Mills Road, North York, Ont., Canada M3C 1V7.

0022-460X/02/030622 + 12 $35.00/0

discussed. Finally, some representative results will be given and tentative conclusions will be drawn.

2. A DYNAMIC MODEL FOR END MILLING AND THE SUGGESTED IMPACT DAMPER

Estimating the cutting forces accurately forms the basis of estimating the dynamic response during machining. A simple model will be discussed here which expresses the tangential cutting force to be proportional with the instantaneous chip thickness. Despite its simplicity, this model captures the essence of the process. Hence,

$$F_T = K_T b t_c, \tag{1}$$

where K_T is the specific cutting force, b is the axial depth of cut and t_c is the instantaneous chip thickness. K_T is generally provided from cutting tests, the empirical parameter representing the material strength and the tool shape. K_T is the specific resistance of the material to be removed. In addition, the radial force may also be expressed in terms of the tangential force as

$$F_R = K_R F_T, \tag{2}$$

where K_R is a proportionality constant. These cutting parameters are illustrated in Figure 1 schematically. In Figure 1, the axial depth of cut, b, is in a normal direction to the plane of the cutter. This cutting force model was first suggested by Koenigsberger and Subberawal [10], then used and enhanced extensively by Tlusty and his various research partners [1, 2, 11–13].

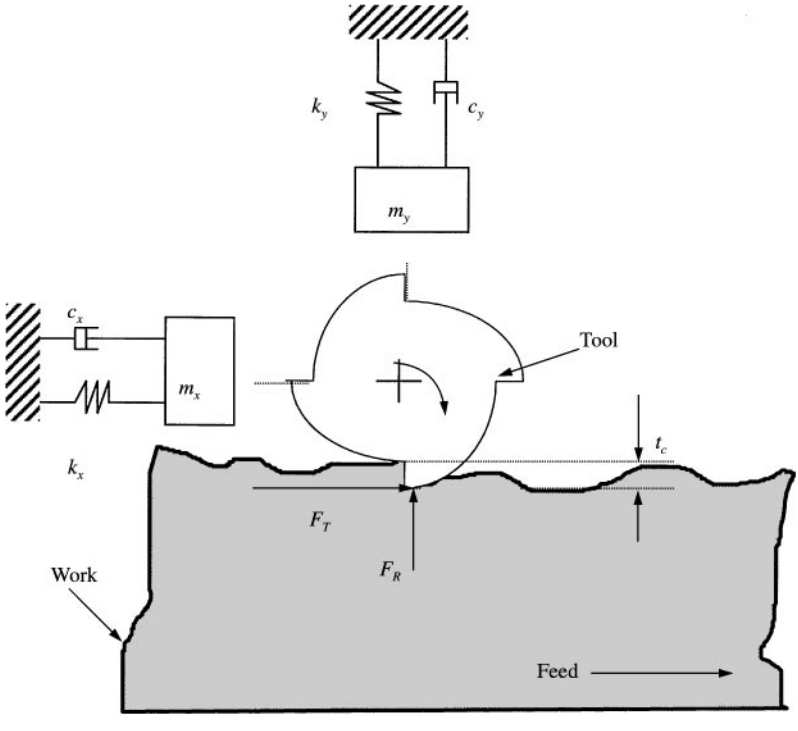

Figure 1. 2-d.o.f. model of the end-milling cutter.

Among the three parameters in equation (1), the chip thickness is the most critical. The chip thickness changes not only with the geometry of the cutting tool and the cutting parameters, but also with the uneven surface left by the previous passes of the cutting tool [2]. Hence, after determining the chip thickness for an uncut fresh surface, this thickness must be compared with the undulations left by the cutting tool during previous passes at the same position (which may significantly alter the thickness of the chip) to obtain the instantaneous thickness of the material left to be removed. The resulting variation induced by the surface waviness from the previous passes, represents the surface regeneration mechanism [2].

There is a possibility of the oscillation amplitude, in the direction away from the workpiece, being greater than the instantaneous chip thickness. This condition results in the tool jumping off the workpiece for a portion of its oscillation cycle. When the tool leaves the workpiece, transient oscillations take place, dissipating energy through structural damping. This basic non-linearity keeps the oscillation amplitudes from growing indefinitely [1, 2]. Once the contact is re-established, forced oscillations resume for the remainder of the cycle.

Oscillations of the flexible cutter may be obtained using a two-degree-of-freedom (2-d.o.f.) model shown in Figure 1. The mass, damping coefficient and stiffness (m, c, k) of this model need to be determined from the modal testing of the structure. Reference [2] is an excellent source for the details of the feedback model summarized here.

The suggested configuration of the impact damper to control the resonance oscillations of the end mill is shown in Figure 2. It is proposed to hollow the core of the cutter and to place an impact damper in the hollow core. The impact damper is simply a cantilevered beam. The dimensional difference between the cavity and the damper results in an

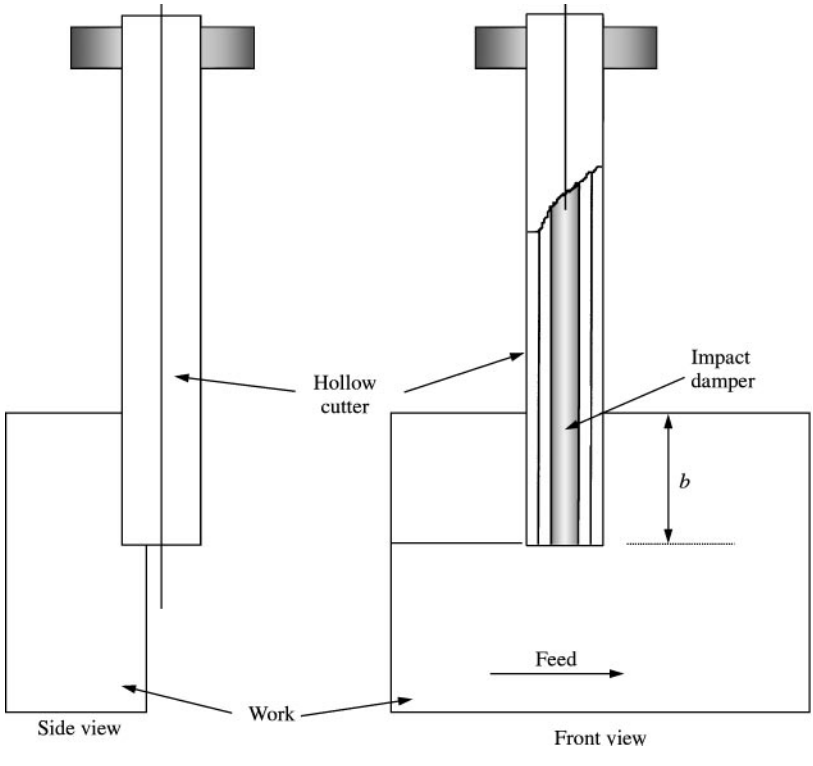

Figure 2. Suggested arrangement of the impact damper and the cutter.

intentional clearance which allows intermittent collisions between the cutter and the impact damper.

Impact damping principle uses the dissipation of energy and exchange of momentum which take place during intermittent collisions. If the clearance is designed properly, the collisions mostly occur when the cutter and the damper move in opposite directions. As a result, the smaller impact damper reverses its direction of motion with the excess momentum it gained. On the other hand, the larger cutter slows down due to the momentum it lost to the damper. This decrease in the speed is expected to lead to a smaller excursion of the cutter. Useful parameters of impact dampers are presented in reference [14] in the form of design charts.

3. NUMERICAL PROCEDURE

A combined mathematical model of the milling cutter and the impact damper beam is shown schematically in Figure 3. In this figure, subscript 1 refers to the cutter, whereas subscript 2 is used for the impact damper. The radial clearance, $d/2$, represents the gap between the inside surface of the hollow cutter and the damper beam. The forces on the cutter are omitted for clarity.

Between collisions, the differential equations of motion of the cutter in the x–y co-ordinate system may be written as

$$\begin{bmatrix} m_{x1} & 0 \\ 0 & m_{y1} \end{bmatrix} \begin{Bmatrix} \ddot{x}_1 \\ \ddot{y}_1 \end{Bmatrix} + \begin{bmatrix} c_{x1} & 0 \\ 0 & c_{y1} \end{bmatrix} \begin{Bmatrix} \dot{x}_1 \\ \dot{y}_1 \end{Bmatrix} + \begin{bmatrix} k_{x1} & 0 \\ 0 & k_{y1} \end{bmatrix} \begin{Bmatrix} x_1 \\ y_1 \end{Bmatrix} = \begin{Bmatrix} F_x \\ F_y \end{Bmatrix}, \tag{3}$$

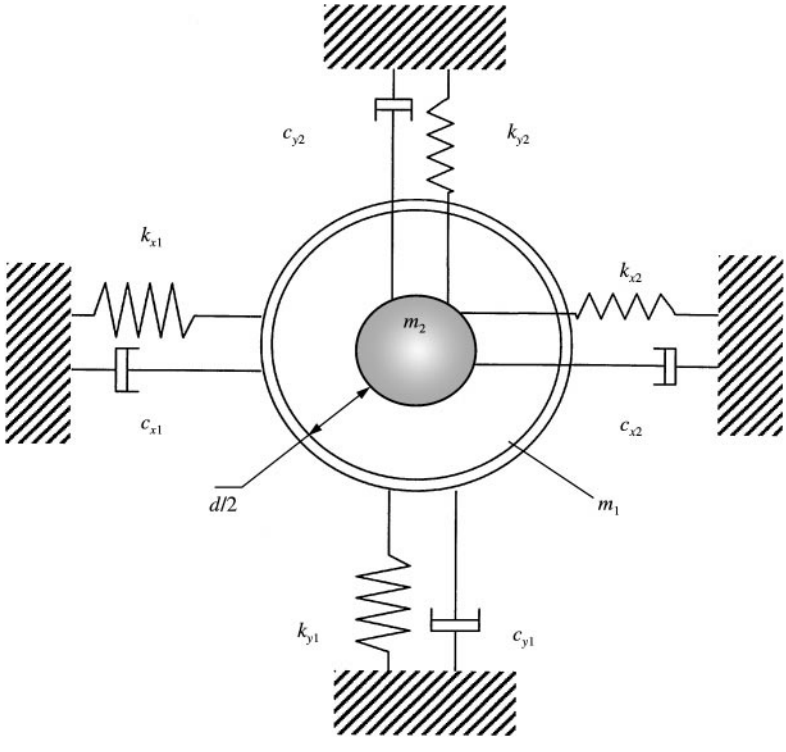

Figure 3. Model of the cutter and the impact damper.

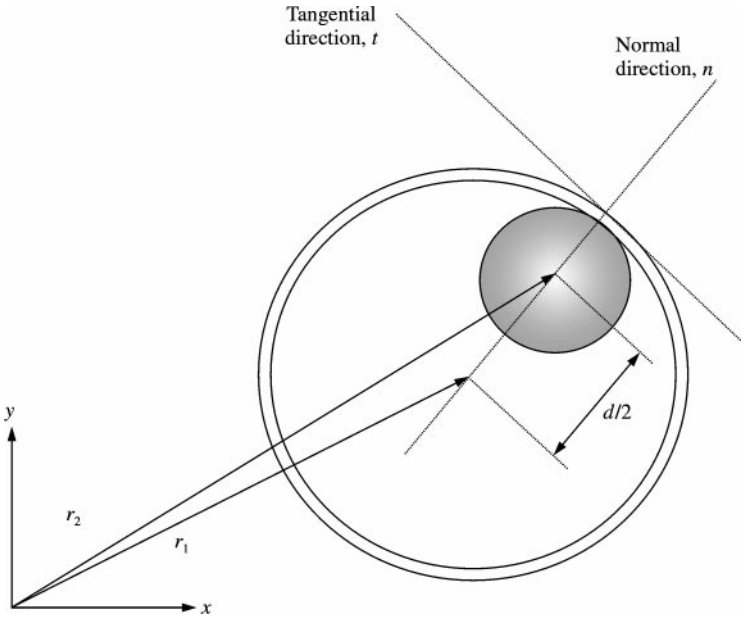

Figure 4. Cutter and the impact damper at an instant of collision.

where an overdot represents differentiation with respect to time. Similarly, for the impact damper

$$\begin{bmatrix} m_{x2} & 0 \\ 0 & m_{y2} \end{bmatrix} \begin{Bmatrix} \ddot{x}_2 \\ \ddot{y}_2 \end{Bmatrix} + \begin{bmatrix} c_{x2} & 0 \\ 0 & c_{y2} \end{bmatrix} \begin{Bmatrix} \dot{x}_2 \\ \dot{y}_2 \end{Bmatrix} + \begin{bmatrix} k_{x2} & 0 \\ 0 & k_{y2} \end{bmatrix} \begin{Bmatrix} x_2 \\ y_2 \end{Bmatrix} = \begin{Bmatrix} 0 \\ 0 \end{Bmatrix}. \tag{4}$$

During simulations, histories of the system co-ordinates were obtained numerically by using a fourth order Runge–Kutta integration procedure [15]. At every solution step, the relative distance was checked to determine the presence of a collision. A contact was obtained when

$$[(x_1 - x_2)^2 + (y_1 - y_2)^2]^{1/2} - d/2 = 0 \tag{5}$$

was satisfied. Numerically, integration of equations (3) and (4) proceeded until a negative value was obtained for the right-hand side in equation (5) which is a collision within the last time step. Then bisection was used to iterate on the time step to determine the instant of collision accurately. A collision was assumed when the absolute value of the left-hand side of equation (5) was obtained to be within 1 millionth of the clearance d. An arbitrary position of the cutter and the damper in contact, is shown in Figure 4. The positions are indicated vectorially with r_1 and r_2. The distance between the two systems is always $d/2$ when in contact.

Instantaneous collisions were assumed between the two systems. The numerical procedure implemented instantaneous changes in the velocities in the normal direction (direction of line of centers) as soon as a collision was detected. The displacements in the normal direction and the co-ordinates in the tangential direction, on the other hand, remained unaffected. New velocities at an instant immediately after a collision, t_+, were obtained in terms of the velocities at the instant just before contact, t_-, by using the

definition of the coefficient of restitution and the conservation of linear momentum

$$e = -(V_{n1+} - V_{n2+})/(V_{n1-} - V_{n2-}),$$

$$m_{n1} V_{n1-} + m_{n2} V_{n2-} = m_{n1} V_{n1+} + m_{n2} V_{n2+}, \tag{6}$$

where subscripts $+$ and $-$ of V_n, indicate velocities at instants t_+ and t_- respectively. Once the new set of initial conditions were obtained at time t_+, integration of equations (3) and (4) resumed until a new contact was detected.

Initial computations were performed using a simplified force model rather than the force feedback model discussed earlier. The purpose of these initial computations was to obtain the optimal combination of the impact damper's parameters to be used in more realistic cutting simulations. A random white noise was used as the excitation in the x direction. The essence of the two-directional cutting forces was preserved by deriving the excitation in the y direction from the same random force. Hence,

$$F_y = K_R F_x, \tag{7}$$

where K_R is the same proportionality constant as in equation (2). The value of 0·3 was used for K_R as this was the empirically obtained value in connection with the modal tests mentioned earlier [2, 12]. Both the cutter and the impact damper were assumed to be axisymmetric having identical parameters in x and y directions. A critical damping ratio of 0·01 was used for both systems, assuming close fitting joints.

4. PARAMETERS OF THE NUMERICAL EXPERIMENTS

The parameters of the system which may affect the performance of the impact damper are (subscripts x and y are omitted for clarity):

(1) *Mass ratio* m_2/m_1: Generally, an impact damper's effectiveness improves with increasing mass ratio [14]. Three mass ratios of 0·1, 0·2 and 0·4 will be used in this investigation.

(2) *Coefficient of restitution of collisions*: Restitution coefficient changes between 0·2 and 0·9 for most engineering materials. Within this range, three values are chosen which approximately represent collisions of hardened smooth surfaces of tool steel (0·8), tool steel with a softer metal-like brass (0·6) and tool steel and hard rubber or teflon surfaces (0·3).

(3) *Natural frequency ratio* ω_2/ω_1: This ratio represents the relative flexibility of the damper beam to that of the cutter for a given mass ratio. Five different values are chosen, namely 0·25, 0·50, 1·00, 1·50 and 2·00.

(4) *Clearance* d: Clearance is the most critical parameter of the impact damper. When d is too large, frequent contacts cannot be established. When d is too small, excessive number of contacts occur, thus effectively having the cutter "carry" the damper rather than collide with it. An optimal clearance is the one which allows intermittent collisions with relatively high approach speeds to take advantage of the momentum exchange fully.

5. RESULTS

Collective results of the simulations performed with the random white noise excitation are shown in Figure 5. In this figure, the vertical axis represents the ratio σ_x/σ_{x0}, where σ_x and σ_{x0} are the root-mean-square (r.m.s.) displacements of the cutter in the x direction with

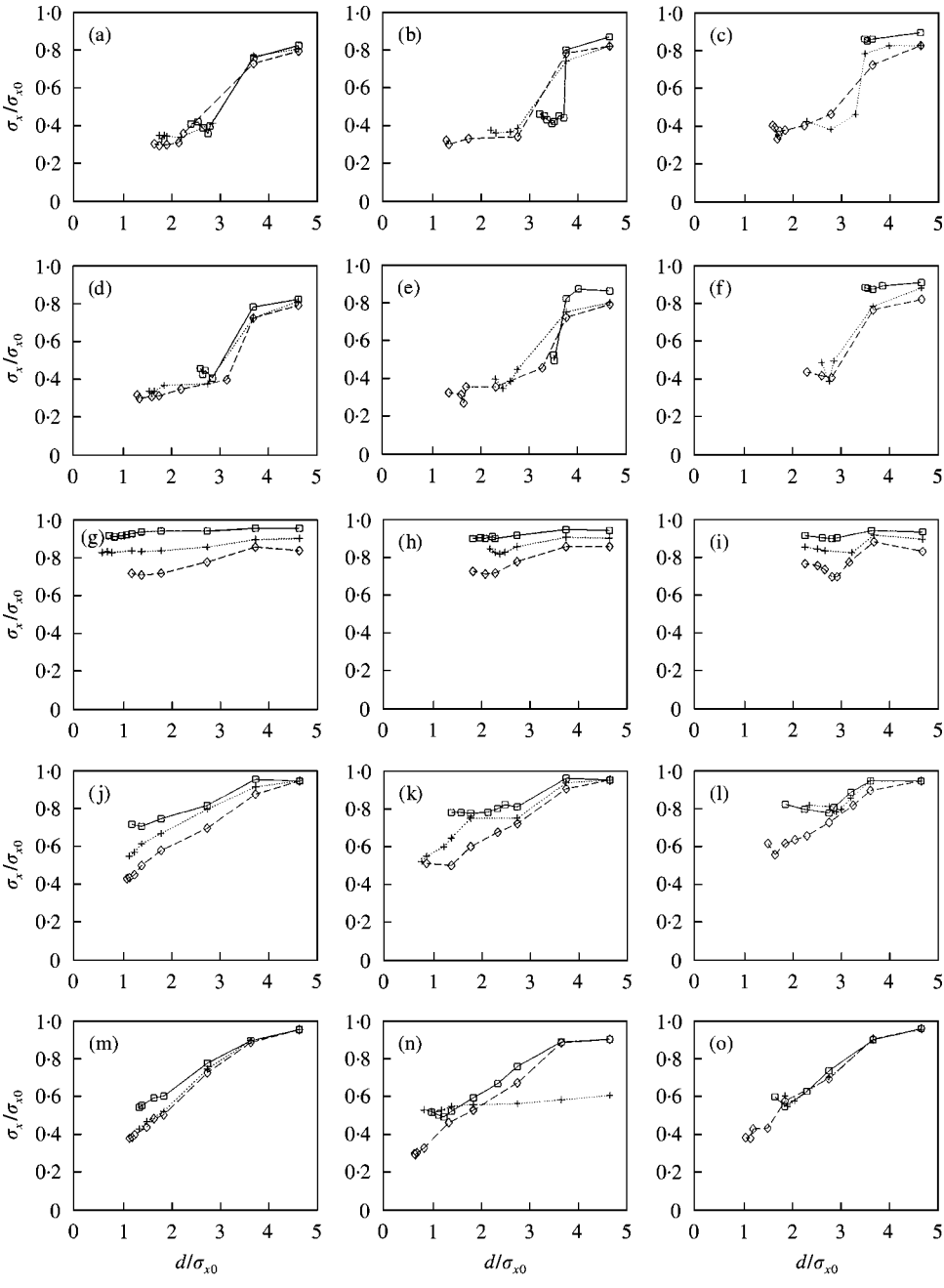

Figure 5. Variation of the r.m.s. reduction ratio with the non-dimensional clearance.

and without the impact damper, respectively. Any value of σ_x/σ_{x0} less than unity represents an attenuation due to the presence of the impact damper. The non-dimensional clearance, d/σ_{x0}, on the other hand, is shown in the horizontal axis. Here d is the total clearance and σ_{x0} is again the r.m.s. displacement of the cutter without impacts. Each column from left to right, corresponds to a coefficient of restitution, e, of 0·3, 0·6 and 0·8. Each row represents a constant value of the natural frequency ratio, ω_2/ω_1, from 0·25 to 2·00. In addition, σ_x/σ_{x0}

values are presented for three different mass ratios, m_2/m_1, of 0·10 (□), 0·20 (+) and 0·40 (◇) in each frame.

In general, smaller values of σ_x/σ_{x0} are obtained when ω_2/ω_1 is smaller than unity. These represent the cases when the impact damper system is more flexible than the cutter. When ω_2/ω_1 is unity, the presence of the impact damper has only a minimal effect. This ineffectiveness may be related to the mostly in-phase motion of the cutter with the damper, due to having the same natural frequency. In-phase motion produces only occasional collisions with small approach speeds, and as a result, relatively ineffective momentum exchange [16].

When ω_2/ω_1 is greater than unity, the trend is to produce smaller σ_x/σ_{x0} for smaller d/σ_{x0}, with an almost linear correlation. These negative-sloped curves represent characteristics approaching that of a rigid barrier instead of an impact damper. It appears that σ_x/σ_{x0} values would become smaller yet, if even smaller d/σ_{x0} than what is presented in Figure 5 were to be tested. These smaller d/σ_{x0} were indeed checked, and an excessive number of collisions were obtained with many consecutive contacts. Eventually, these smaller clearances would produce results approaching the case of the cutter carrying the impact damper. The smallest d/σ_{x0} in Figure 5, represents the threshold of reasonably well-separated collisions between the two systems.

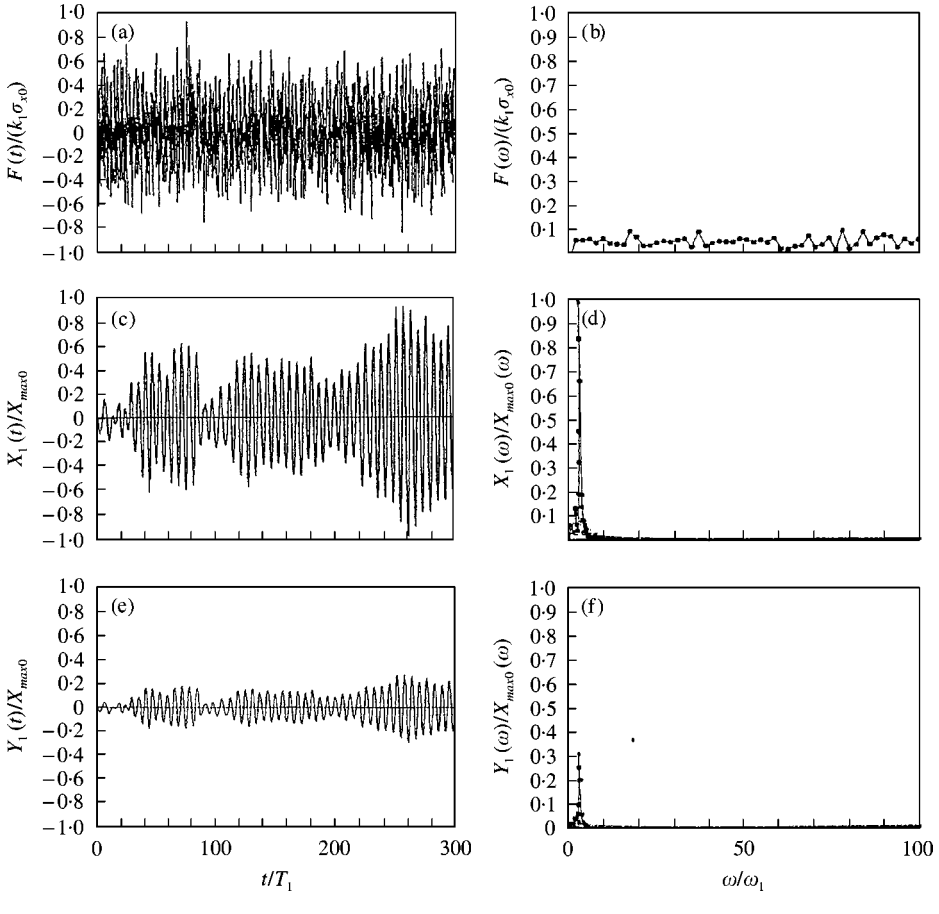

Figure 6. Histories of the (a) excitation, and the displacement of the cutter without impacts in (a) x direction and (b) y direction. (b), (d) and (f) correspond to the FFT of the histories in the first column.

Generally, increasing the mass ratio m_2/m_1 produces favourable results. Smallest of σ_x/σ_{x0} are always obtained for the largest m_2/m_1. In addition, for the two smallest ω_2/ω_1 in the first two rows, the variation of σ_x/σ_{x0} with the clearance becomes less pronounced around the optimum value of the clearance, as the mass ratio increases. This last trend is particularly important practically suggesting relative insensitivity to the clearance.

Finally, the favourable effect of increasing the mass ratio seems to diminish from 0·20–0·40 as compared to 0·10–0·20. Hence, increase of the mass ratio beyond 0·40 may not produce a proportional return in the performance of the impact damper.

Results in the first column of Figure 5, for $e = 0{\cdot}3$, show higher attenuations as compared to those of the other two columns, for $e = 0{\cdot}6$ and 0·8. A mass ratio of 0·20 or 0·40, for

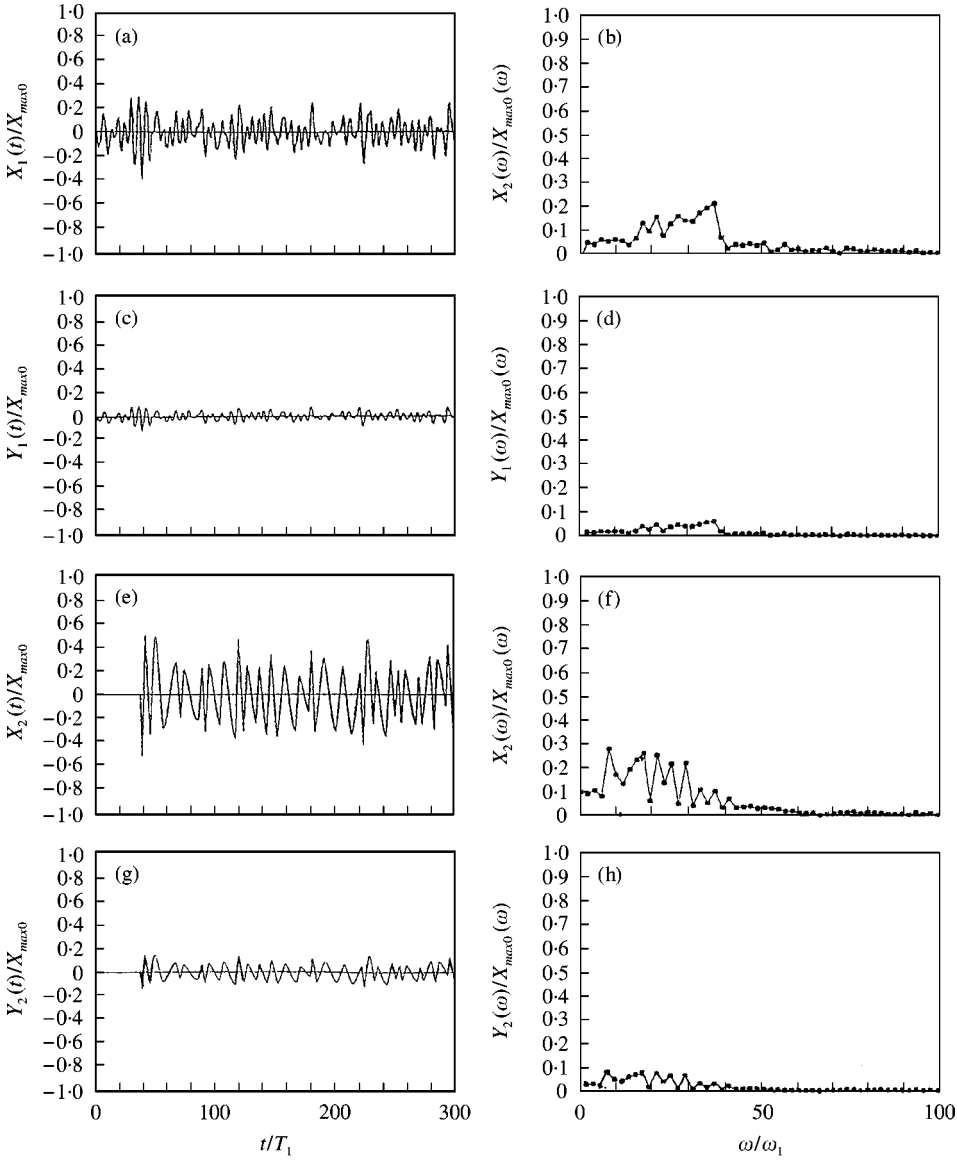

Figure 7. Histories of the displacement of the cutter in (a) x direction and (c) y direction; and the displacement of the impact damper in (e) x direction and (g) y direction. (b), (d), (f) and (h) correspond to the FFT of the histories in the first column. $e = 0{\cdot}3$, $m_2/m_1 = 0{\cdot}4$, $\omega_2/\omega_1 = 0{\cdot}25$ and $d/\sigma_{x0} = 1{\cdot}75$.

a range of non-dimensional clearances from approximately 1·50–2·25 and for a frequency ratio of ω_2/ω_1 of 0·25, can produce a σ_x/σ_{x0} of approximately 0·30, representing a 70% attenuation.

The histories of the random force and the displacement of the cutter in x and y directions without the impact damper, are presented, in Figure 6(a), 6(c) and 6(e). The second column of Figure 6 represents the fast Fourier transformation (FFT) of the histories in the first column. The non-dimensionalizing parameters for the vertical axes k_1, σ_{x0}, X_{max0} and $X_{max0}(\omega)$ are the stiffness of the cutter, its r.m.s. displacement without collisions, its peak displacement amplitude (time) and its peak spectral amplitude respectively. Horizontal axes

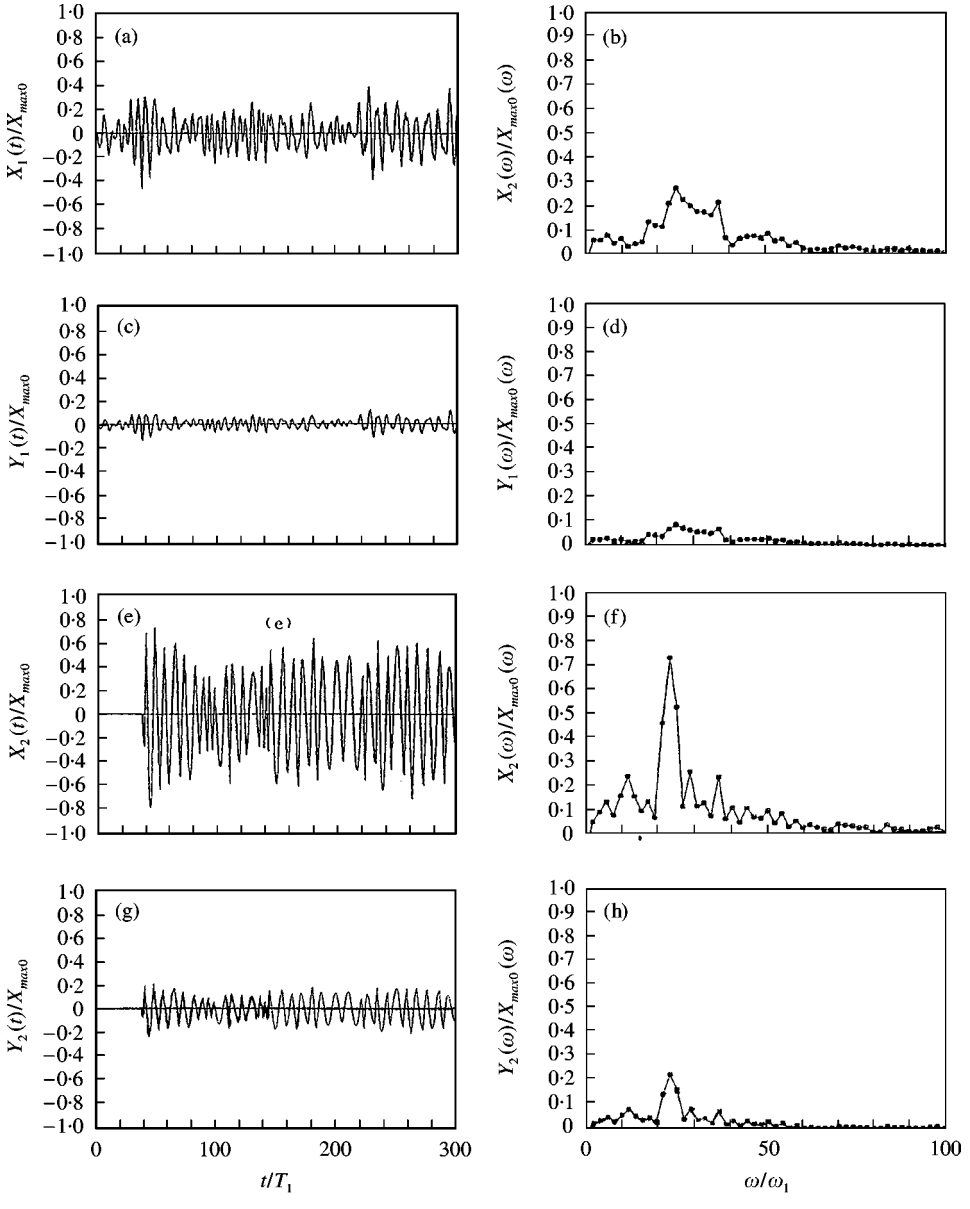

Figure 8. Same as in Figure 7 but $e = 0{\cdot}8$, $m_2/m_1 = 0{\cdot}4$, $\omega_2/\omega_1 = 0{\cdot}25$ and $d/\sigma_{x0} = 1{\cdot}60$.

are non-dimensionalized by dividing time with the natural period (T_1), and frequency with the natural frequency of the cutter (ω_1).

In Figure 6(d) and 6(f), the resonance of the cutter is quite apparent without the impact damper. The wideband random force, produces a narrowband response of the cutter due to light structural damping. The same format in Figure 6 is preserved for presenting the results with the impact damper in Figures 7 and 8.

In Figure 7, the displacement of the cutter and the impact damper in two directions are presented for $e = 0{\cdot}3$, $m_2/m_1 = 0{\cdot}4$, $\omega_2/\omega_1 = 0{\cdot}25$ and $d/\sigma_{x0} = 1{\cdot}75$. In comparison with the results in Figure 6, the presence of collisions produces at least 2·5 times smaller displacement peaks in the x direction. In addition, with the presence of collisions, the spectral content of the displacement is now wider with considerably smaller amplitudes. This phenomenon is due to the presence of the intermittent discontinuities which increase the contribution of the high-frequency components. The same comments are mostly valid for the results in Figure 8 for the higher coefficient of restitution of $e = 0{\cdot}8$, $m_2/m_1 = 0{\cdot}4$, $\omega_2/\omega_1 = 0{\cdot}25$ and $d/\sigma_{x0} = 1.60$.

6. CONCLUSIONS

Some representative results are presented to numerically predict the effectiveness of an impact damper in controlling the excessive oscillations of a long end milling cutter. Essential features of a feedback model is described here for the cutting force. However, the preliminary results are for a randomly excited cutter with no feedback. Results of the initial computations are encouraging. It may indeed be possible to prevent the initiation of the self-excited chatter vibrations using a simple impact damper arrangement. However, before such claims, predicted performance of the model should certainly be verified with a more realistic force feedback model, and with experimental observations.

Although not reported here, the suggested impact damper has also been found to be effective in reducing transient oscillations of the cutter, after the cutter is given an initial velocity. Considering the intermittent nature of the milling process, this feature is significant for chatter suppression.

REFERENCES

1. J. TLUSTY and F. ISMAIL 1982 *Annals of CIRP* **30**, 229–304. Basic nonlinearity in machining chatter.
2. J. TLUSTY 1985 in *Handbook of High-Speed Machining Technology* (R. I. King, editor), 48–154 New York: Chapman & Hall Ltd. Machine dynamics.
3. Y. S. TARNG, H. T. YOUNG and B. Y. LEE 1994 *International Journal of Machine Tools and Manufacturing* **34**, 183–197. An analytical model of chatter vibration in metal cutting.
4. H. OTA and K. KONO 1974 *American Society of Mechanical Engineers, Journal of Engineering for Industry* **96**, 1337. On chatter vibrations of machine tool or work due to regenerative effect and time lag.
5. S. KATO and E. MARUI 1974 *American Society of Mechanical Engineers, Journal of Engineering for Industry* **96**, 179–185. On the cause of regenerative chatter due to workpiece deflections.
6. B. Y. LEE, Y. S. TARNG and S. C. MA 1995 *International Journal of Machine Tools Manufacturing* **35**, 951–962. Modelling of the process damping force in chatter vibration.
7. S. C. LIN, R. E. DEVOR and S. G. KAPOOR 1990 *Transactions of American Society of Mechanical Engineers, Journal of Engineering for Industry* **112**, 1–11. The effects of variable cutting speed on vibration control in face milling.
8. S. C. LIN and M. R. HU 1992 *International Journal of Machine Tools and Manufacturing* **32**, 629–640. Low vibration control system in turning.

9. Z. MEI, S. YANG, H. SHI, S. CHANG and K. F. EHMANN 1994 *International Journal of Machine Tools Manufacturing* **34**, 981–990. Active chatter suppression by on-line variation of the rake and clearance angles in turning—principles and experimental investigations.
10. F. KOENIGSBERGER and A. J. P. SABERWAL 1966 *International Journal of Machine Tool Design Research* **1**. An investigation into the cutting force pulsation during milling operations.
11. J. TLUSTY and P. MACNEIL 1975 *Annals of CIRP* **24**, 21–29. Dynamics of cutting in end milling.
12. F. M. ISMAIL 1982 *Ph.D. Thesis, Mechanical Engineering Department, McMaster University*. Identification, modelling and modification of mechanical structures from modal analysis testing.
13. J. TLUSTY 1986 *American Society of Mechanical Engineers Journal of Engineering for Industry* **108**, 59–67. Dynamics of high speed milling.
14. C. N. BAPAT and S. SANKAR 1985 *Journal of Sound and Vibration* **99**, 85–94. Single unit damper in free and forced vibration.
15. S. S. RAO 1980 *Mechanical Vibrations*. Don Mills, Ontario: Addison-Wesley, Co.; first edition.
16. L. A. CHEN and S. E. SEMERCIGIL 1992 *Journal of Sound and Vibration* **157**, 303–315. A beam impactor.